Crystal Structures of Tris[*N*-(4-methylphenyl)acetohydroxamato]iron(III)–Acetone (1/1) and Tris(*N*-methyl-4-methylbenzohydroxamato)iron(III) [and gallium(III)]–Acetone–Water (1/1/1).† Structure–Stability Relationships for the Hydroxamate Complexes of Fe^{3+} and Ga^{3+}

Andreas Dietrich,[a] Krzysztof A. Fidelis,[a] Douglas R. Powell,[a] Dick van der Helm *,[a] and D. Larry Eng-Wilmot[b]

[a]*Department of Chemistry and Biochemistry, The University of Oklahoma, Norman, OK 73019-0370, USA*
[b]*Department of Chemistry, Rollins College, Winter Park, FL 32789, USA*

Accurate molecular structures of iron(III) and gallium(III) complexes of structurally related model hydroxamic acids were investigated by single-crystal X-ray diffraction at −135(2) °C: $[Fe(mpa)_3]\cdot Me_2CO$ **1** [mpa = *N*-(4-methylphenyl)acetohydroxamate], monoclinic, space group $P2_1/a$, a = 10.635(3), b = 12.137(2), c = 23.667(6) Å, β = 102.34(2)°, Z = 4, R = 0.030 for 5115 reflections; $[Fe(mmb)_3]\cdot H_2O\cdot Me_2CO$ **2** (mmb = *N*-methyl-4-methylbenzohydroxamate), monoclinic, space group $P2_1/a$, a = 10.852(2), b = 30.690(6), c = 10.494(2) Å, β = 117.89(2)°, Z = 4, R = 0.034 for 6381 reflections; $[Ga(mmb)_3]\cdot H_2O\cdot Me_2CO$ **3**, monoclinic, space group $P2_1/a$, a = 10.822(4), b = 30.718(14), c = 10.463(5) Å, β = 118.51(3)°, Z = 4, R = 0.036 for 6 333 reflections. All three complexes crystallize in their enantiomeric Λ- and Δ-*cis* configurations. Structural differences between **1** and **2** were used to develop a set of structural criteria to establish the relative stability of the two compounds. These criteria were then applied to compounds **2** and **3** leading to the conclusion that the gallium(III) complex is thermodynamically more stable than the iron(III) complex. It is shown, however, that when the large differences in the free energy of formation for the aqueous ions are taken into account these conclusions are in agreement with the thermodynamic observations that the formation constant of the iron(III) hydroxamate complex is larger than that of its isomorphous gallium(III) complex, and that Fe^{3+} displaces Ga^{3+} in hydroxamato complexes of the latter.

Facultative fungi elaborate low-molecular-weight (*e.g.* 500–1000) cyclic and linear trihydroxamic acid-type siderophores, derived from either derivatized N^{δ}-hydroxyornithine (ferrichromes, fusarinines, coprogens) or 1-amino-ω-hydroxyaminoalkanes (ferrioxamines) to facilitate Fe^{3+} acquisition by the micro-organism and stereospecific transport across the cell membrane.[1–4] The central feature underlying the important chemical and biological properties[5] of these secondary hydroxamic acids, of the form $R^1C(O)N(OH)R^2$ (where R^1 and $R^2 \neq H$), is their ability to form, with unusual high selectivity, octahedral complexes with the spherically symmetric trivalent Fe^{3+} cation with high thermodynamic stability. This is reflected in the values of the formation constants for either the 1:1 complexes, with an hexadentate ligand (K_f/dm^3 mol^{-1}), or 3:1 complexes with bidentate ligands (β_3/dm^9 mol^{-3}) which fall in the range of 10^{28}–10^{32}.[6] Other highly charged small cations like Ga^{3+} and Al^{3+} also form stable complexes with hydroxamates but their formation constants are smaller.[3,6,7] The selectivity of this unsymmetrical bidentate ligand for Fe^{3+} ion (as opposed to Fe^{2+} and other biologically important divalent cations) is a function of: (1) the strong electrostatic bonding interactions of the hydroxamate oxygen atoms with the trivalent Fe^{3+} ion; (2) the structural geometry of the ligand; and (3) the small ionic radius of the Fe^{3+} ion. The variations in the thermodynamic stability between different iron(III) trihydroxamates are dependent upon: (1) the local electronic influences (inductive and resonance) of the hydroxamate substituents on electron delocalization within the chelate ring; and (2) structural and steric constraints imposed by the ligand.

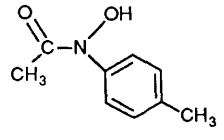

Hmpa

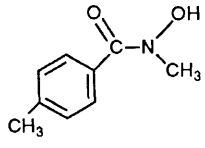

Hmmb

The structures of a number of natural hydroxamate siderophores have been determined by single-crystal X-ray diffraction.[8] The accuracy of these structures is limited due to the large molecular size. Therefore, another approach to establish a relationship between structure and thermodynamic stability has been the study of smaller model tris(hydroxamato) complexes of Fe^{3+}.[9–11] In this study, as a follow up to a recently reported comparison of the ligands,[12] we report the molecular structures of the iron(III) complexes of two model hydroxamic acids, *N*-(4-methylphenyl)acetohydroxamic acid (Hmpa) and *N*-methyl-4-methylbenzohydroxamic acid (Hmmb) in which the hydroxamate R groups have been interchanged, as well as the isomorphous gallium(III) complex of Hmmb. The structures of the iron(III) complexes are compared, which allows the establishment of a number of structural and electronic criteria which correlate with their thermodynamic stability. These criteria are subsequently used to analyse the relative stability of the gallium(III) and iron(III) complexes with mmb.

Results and Discussion

General Description of the Structures.—The ORTEP

† *Supplementary data available:* see Instructions for Authors, *J. Chem. Soc., Dalton Trans.*, 1991, Issue 1, pp. xviii–xxii.

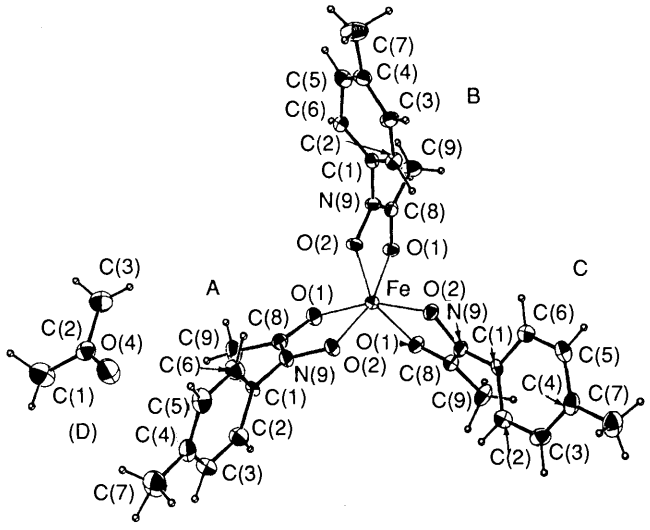

Fig. 1 A single molecule of $[Fe(mpa)_3]$ with 50% probability thermal ellipsoids and atom numbering scheme: A–C are the three ligands and D is the acetone molecule

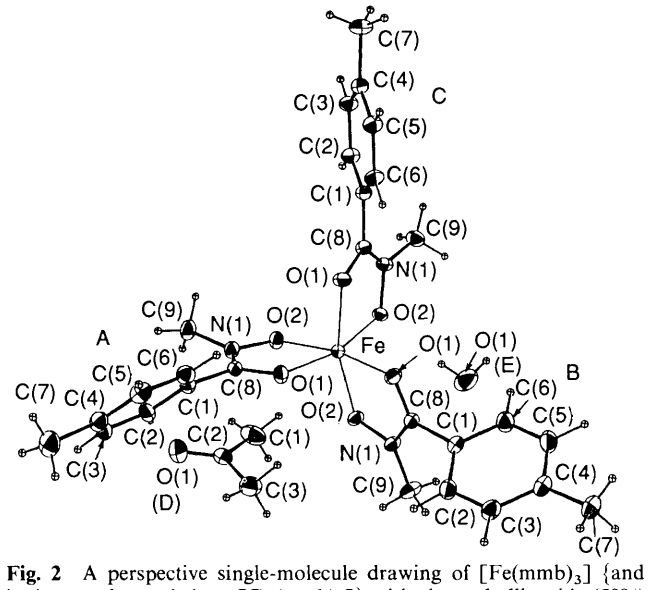

Fig. 2 A perspective single-molecule drawing of $[Fe(mmb)_3]$ {and its isomorphous chelate, $[Ga(mmb)_3]$} with thermal ellipsoids (50%) and atom numbering scheme. Symbols as in Fig. 1

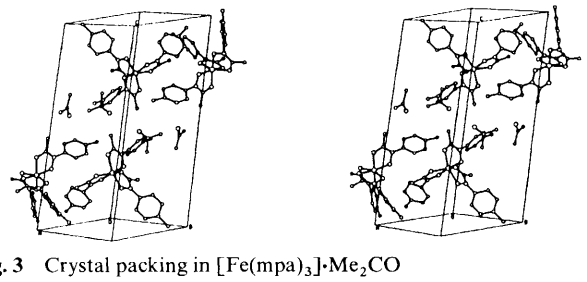

Fig. 3 Crystal packing in $[Fe(mpa)_3]\cdot Me_2CO$

drawings of single molecules of $[Fe(mpa)_3]\cdot Me_2CO$ **1** and $[Fe(mmb)_3]\cdot H_2O\cdot Me_2CO$ **2** are given, along with the appropriate atom numbering schemes, in Figs. 1 and 2, respectively {the structure of $[Ga(mmb)_3]\cdot H_2O\cdot Me_2CO$ **3** is isomorphous with that of **2**}. In **1** and **2** each unsymmetric bidentate hydroxamate group assumes the *cis* (*fac*) configuration about the metal ion, with the trigonal octahedral faces (related by a pseudo three-fold axis) formed by the carbonyl oxygen O(1-A,B,C) and the oxime oxygen O(2-A,B,C) atoms, being nearly parallel. This arrangement places the aliphatic methyl groups on one side of the molecule while the aromatic 4-methylphenyl substituents are oriented toward the opposite side. In each structure the symmetry imposed by the crystallographic inversion centre results in both enantiomeric Λ- and Δ-*cis* configurations at the metal-ion co-ordination site.

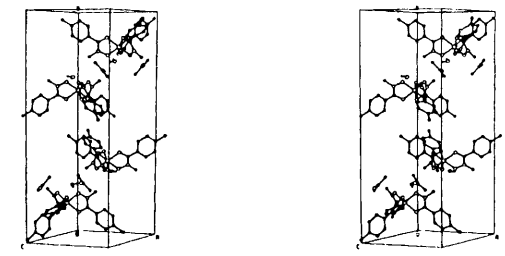

Fig. 4 Crystal packing in $[Fe(mmb)_3]\cdot H_2O\cdot Me_2CO$ [and its isomorphous gallium(III) chelate]

Crystallographic data, atomic coordinates, and bond distances and selected bond and torsion angles for the three compounds are presented in Tables 1–5. The average dimensions of the five-membered iron(III) hydroxamate chelate rings of **1** and **2**, discussed in detail below, fall within the range expected for natural siderophores[8] and model iron(III) hydroxamate compounds;[9–11] the dimensions of **3** are similar to those reported for a tris(benzohydroxamato)gallium(III) complex.[13]

In complex **1**, while the average Fe–O(1) distance is 2.054(1) Å, individual values for each of the hydroxamate rings labelled A–C are in the range 2.037(1)–2.067(1) Å; these bond distances, expected to be similar because of the near equality of all other equivalent bond distances and angles, are significantly different. Analysis of the close contacts within the structure indicates at least twelve 2.5–3.0 Å contacts between co-ordinating oxygen atoms and hydrogen atoms from neighbouring molecules. These contacts could lead to this inconsistency in the Fe–O(1) distances. The crystal packing for **1** (Fig. 3) indicates that the acetone molecule does not make any close intermolecular contacts.

In the crystal packing of complex **2** (Fig. 4) the acetone molecule shows no important intermolecular contacts, but the water solvate molecule is involved in a hydrogen bond with the oxime oxygen, atom O(2C) [H(2E)···O(2C) 2.05(3) Å]. This interaction results in a lengthening of the Fe–O(2C) bond [1.995(1) Å] by approximately 0.02 Å, as compared to the average Fe–O(2A,B) distance of 1.977(1) Å. It has been suggested from kinetic studies that, in aqueous solution, dissociation of the hydroxamate group from the central Fe^{3+} ion is initiated at the oxime oxygen.[14] This idea finds support in these X-ray results, which indicate that the O(2) atom is the preferred site for hydrogen bonding and protonation, owing to the larger basicity of the N(9)–O(2) *versus* C(8)–O(1) oxygen atoms. In structure **2**, the interplanar angle formed between the phenyl and hydroxamate planes in ligand B (71.5°) is significantly different from that observed for ligands A and C (40.0 and 47.1°, respectively). A close contact [3.14(2) Å] between the phenyl ring and the water molecule [H(6B)···O(1E)] suggests that the conformational angle for the C(1)–C(8) bond in ligand B is determined by this contact.

The crystal structure of complex **3** is isomorphous with that of **2**. A similar lengthening by 0.02 Å in the Ga–O(2C) distance [1.966(2) Å] compared to an average of 1.945(2) Å for Ga–O(2-A,B) is observed and attributed to a 1.99(4) Å hydrogen bond between the water solvate molecule and O(2C) [O(2C)···H(2E)], as observed in **2**. The dihedral angle between the phenyl and hydroxamate planes in ligand B is 68.8° (71.5° in **2**), and results from a 3.01(3) Å contact H(6B)···O(1E), which hinders rotation about the C(1)–C(8) bond.

Table 1 Summary of crystallographic data for [Fe(mpa)$_3$] **1**, [Fe(mmb)$_3$] **2** and [Ga(mmb)$_3$] **3***

	1	**2**	**3**
Formula	$C_{27}H_{30}FeN_3O_6 \cdot C_3H_6O$	$C_{27}H_{30}FeN_3O_6 \cdot H_2O \cdot C_3H_6O$	$C_{27}H_{30}GaN_3O_6 \cdot H_2O \cdot C_3H_6O$
M	606.5	624.5	638.4
Crystal size/mm	0.35 × 0.25 × 0.20	0.64 × 0.30 × 0.62	0.23 × 0.16 × 0.15
Cell parameters			
a/Å	10.635(3)	10.852(2)	10.822(4)
b/Å	12.137(2)	30.690(6)	30.718(14)
c/Å	23.667(6)	10.494(2)	10.463(5)
β/°	102.34(2)	117.89(2)	118.51(3)
U/Å^3	2 984.3	3 089.1	3 056.4
D_c/g cm^{-3}	1.35	1.34	1.385
μ(Mo-Kα)/cm^{-1}	5.04	4.92	9.65
F(000)	1 264	1 304	1 324
$2\theta_{max}$/°	50	53	53
Scan width/°	0.75 + 0.25 tan θ	0.80 + 0.20 tan θ	1.00 + 0.35 tan θ
Horizontal aperture/mm	2.50 + 0.86 tan θ	2.00	2.5
t_{max}/s	45	60	120
Total measurements	5 115	6 381	6 333
No. observed reflections [$I \geqslant 2\sigma(I)$]	4 677	5 432	4 968
R	0.030	0.034	0.036
R'	0.033	0.044	0.042

* Details in common: monoclinic; space group $P2_1/a$; $Z = 4$; Mo-Kα radiation (λ = 0.7107 Å); vertical aperture 6.00 mm; 138 ± 2 K; $w = 1/\sigma_F^2$ where σ_F was from counting statistics.

Table 2 Positional parameters for [Fe(mpa)$_3$] and solvent acetone (D) molecules; estimated standard deviations (e.s.d.s) are given in parentheses

Atom	x	y	z	Atom	x	y	z
Fe	0.091 76(2)	−0.013 46(2)	0.266 03(1)	C(4B)	0.134 8(2)	0.438 1(2)	0.101 9(1)
O(1A)	0.148 8(1)	0.015 1(1)	0.352 5(1)	C(5B)	0.236 0(2)	0.434 7(2)	0.149 6(1)
O(2A)	−0.075 0(1)	0.004 1(1)	0.288 9(1)	C(6B)	0.257 8(2)	0.343 1(2)	0.185 4(1)
N(9A)	−0.061 3(1)	0.036 2(1)	0.346 1(1)	C(7B)	0.108 0(2)	0.542 0(2)	0.066 3(1)
O(1B)	0.280 1(1)	0.011 8(1)	0.259 0(1)	C(8B)	0.291 8(2)	0.093 8(2)	0.227 4(1)
O(2B)	0.080 8(1)	0.133 1(1)	0.229 9(1)	C(9B)	0.414 2(2)	0.115 2(2)	0.208 2(1)
N(9B)	0.191 1(1)	0.159 5(1)	0.210 8(1)	C(1C)	−0.080 6(2)	−0.246 8(2)	0.147 8(1)
O(1C)	0.143 8(1)	−0.176 3(1)	0.278 4(1)	C(2C)	−0.163 3(2)	−0.328 3(2)	0.159 2(1)
O(2C)	0.006 3(1)	−0.080 2(1)	0.191 8(1)	C(3C)	−0.247 7(2)	−0.378 0(2)	0.113 6(1)
N(9C)	0.007 4(1)	−0.194 1(1)	0.193 9(1)	C(4C)	−0.253 3(2)	−0.346 3(1)	0.056 7(1)
C(1A)	−0.179 7(2)	0.058 5(2)	0.363 7(1)	C(5C)	−0.172 0(2)	−0.262 2(2)	0.046 6(1)
C(2A)	−0.218 1(2)	−0.006 7(2)	0.404 8(1)	C(6C)	−0.086 1(2)	−0.212 4(2)	0.091 4(1)
C(3A)	−0.334 8(2)	0.014 1(2)	0.419 9(1)	C(7C)	−0.348 2(2)	−0.398 8(2)	0.007 4(1)
C(4A)	−0.415 0(2)	0.098 3(2)	0.394 1(1)	C(8C)	0.085 9(2)	−0.239 8(2)	0.238 7(1)
C(5A)	−0.373 9(2)	0.163 2(2)	0.353 3(1)	C(9C)	0.111 1(2)	−0.361 0(2)	0.242 1(1)
C(6A)	−0.257 7(2)	0.143 9(2)	0.337 8(1)				
C(7A)	−0.544 1(2)	0.117 8(2)	0.409 4(1)	Solvent			
C(8A)	0.057 7(2)	0.039 3(2)	0.377 3(1)	C(1D)	0.058 3(3)	0.285 0(3)	0.638 9(1)
C(9A)	0.085 2(2)	0.070 2(2)	0.439 6(1)	C(2D)	0.065 9(2)	0.272 4(2)	0.577 0(1)
C(1B)	0.178 3(2)	0.251 9(2)	0.172 3(1)	C(3D)	0.182 6(3)	0.317 2(3)	0.559 7(1)
C(2B)	0.079 2(2)	0.251 4(2)	0.123 5(1)	O(4D)	−0.017 9(2)	0.226 4(2)	0.542 8(1)
C(3B)	0.058 1(2)	0.344 2(2)	0.088 7(1)				

Structural Changes in the Hydroxamic Acids upon Iron(III) Chelation.—Several important changes are observed in the structure and conformation of the hydroxomate ligating group of the ligands, mpa and mmb, as they undergo deprotonation and complexation reactions. Structurally, the hydroxamate group in each ligand undergoes a configurational change from the *trans* geometry [12] to the *cis* configuration required to form the five-membered chelate rings. This change is also accompanied by a twist of the 4-methylphenyl group out of the hydroxamate plane. In the ligand mpa the aromatic ring is nearly coplanar with the hydroxamate group, exhibiting a dihedral angle of 11°,[12] while in its iron(III) chelate the substituent rings are twisted from the plane in opposite directions, as seen in the angle O(2)–N(9)–C(1)–C(6) (Table 5: Ligand C, 47.3; ligands A and B, −63.0 and −53.6°, respectively). In the structure of mmb [12] the phenyl ring is not coplanar with the hydroxamate group (interplanar angle 34°), and in [Fe(mmb)$_3$] and its gallium analogue the phenyl rings are once again twisted from the hydroxamate plane, with ring B oriented in one direction (−65.3°), and rings A and C in the other (40.0 and 42.5°, respectively, Table 5).

Dimensionally, several significant changes occur in the hydroxamate C–N, C=O and N–O bonds as a result of metal chelation. The hydroxamate carbonyl C(8)–O(1) bond becomes significantly longer by 0.030 Å in complex **1** [from 1.238(2) Å in Hmpa to an average of 1.268(2) Å in [Fe(mpa)$_3$]} and 0.034 Å in **2** [a change from 1.244(2) to 1.278(2) Å, respectively]. At the same time the C(8)–N(9) bond decreases in length by 0.032 Å in **1** [1.356(2) to 1.324(2) Å] and 0.025 Å in **2** [1.340(2) to 1.315(2) Å]. Metal-ion co-ordination also brings about a shortening of the oxime N(9)–O(2) bond by 0.016 Å in **1** and by 0.027 Å in **2**. Similar changes in the hydroxamate dimensions have been observed in the molecular structures of the deferriferrioxamine E–ferrioxamine E [15,16] and the *N*-(4-cyanophenyl)acetohydroxamic acid–tris[*N*-(4-cyanophenyl)acetohydroxamato]iron(III) [9] ligand–chelate pairs. Lastly, in general, the small changes in the lengths of the bonds made between the R substituents and the hydroxamate C(8)–N(9) atoms upon metal co-ordination emphasize the low degree of involvement of the 4-methylphenyl group on the electronic stabilization of the chelate, see below. As expected,

Table 3 Atomic coordinates for the non-hydrogen atoms in $[Fe(mmb)_3]$ and $[Ga(mmb)_3]$ (given on the lower line) and the solvent molecules [acetone (D) and water (E)]; e.s.d.s are given in parentheses

Atom	*x*	*y*	*z*
Fe	0.190 31(2)	0.155 30(1)	0.511 82(2)
Ga	0.194 92(3)	0.156 43(1)	0.512 63(3)
O(1A)	0.162 8(1)	0.116 07(4)	0.654 0(1)
	0.159 3(2)	0.118 43(6)	0.645 6(2)
O(1B)	0.048 4(1)	0.118 42(4)	0.345 8(1)
	0.060 4(2)	0.121 23(6)	0.344 4(2)
O(1C)	0.343 9(1)	0.115 61(4)	0.516 9(1)
	0.349 3(2)	0.117 68(6)	0.529 6(2)
O(2A)	0.303 6(1)	0.185 82(4)	0.696 4(1)
	0.308 8(2)	0.187 30(6)	0.694 0(2)
O(2B)	0.020 9(1)	0.191 49(4)	0.445 8(1)
	0.029 4(2)	0.192 92(6)	0.451 6(2)
O(2C)	0.269 6(1)	0.191 73(4)	0.410 4(1)
	0.268 8(2)	0.193 02(6)	0.410 3(2)
N(9A)	0.308 1(1)	0.163 94(5)	0.813 2(1)
	0.313 2(1)	0.164 42(7)	0.809 4(2)
N(9B)	−0.092 9(1)	0.172 90(5)	0.332 5(1)
	−0.085 1(2)	0.173 36(7)	0.339 4(2)
N(9C)	0.386 1(1)	0.173 14(5)	0.412 5(1)
	0.385 5(2)	0.173 39(7)	0.413 9(2)
C(1A)	0.218 9(2)	0.103 40(6)	0.899 6(2)
	0.220 8(2)	0.104 29(8)	0.893 5(3)
C(2A)	0.203 4(2)	0.123 91(6)	1.010 2(2)
	0.207 3(3)	0.124 43(9)	1.005 8(3)
C(3A)	0.183 6(2)	0.099 19(7)	1.109 8(2)
	0.187 6(3)	0.099 4(1)	1.105 1(3)
C(4A)	0.178 5(2)	0.054 01(7)	1.101 8(2)
	0.180 8(3)	0.054 26(9)	1.095 0(3)
C(5A)	0.193 8(2)	0.033 92(6)	0.991 0(2)
	0.195 1(3)	0.034 38(9)	0.982 3(3)
C(6A)	0.212 2(2)	0.058 22(6)	0.889 8(2)
	0.213 7(3)	0.059 22(9)	0.882 0(3)
C(7A)	0.152 1(2)	0.027 65(8)	1.207 9(2)
	0.153 8(4)	0.027 5(1)	1.200 0(4)
C(8A)	0.231 5(3)	0.128 49(6)	0.785 0(2)
	0.232 8(3)	0.129 78(8)	0.778 6(3)
C(9A)	0.417 7(2)	0.179 47(6)	0.951 2(2)
	0.425 2(3)	0.178 6(1)	0.949 8(3)
C(1B)	−0.187 5(2)	0.114 20(5)	0.156 3(2)
	−0.180 1(3)	0.115 05(8)	0.159 3(3)
C(2B)	−0.297 5(2)	0.093 36(7)	0.164 6(2)
	−0.289 4(3)	0.094 55(9)	0.170 1(3)
C(3B)	−0.396 1(2)	0.070 92(6)	0.047 1(2)
	−0.390 2(3)	0.071 25(9)	0.052 4(3)
C(4B)	−0.389 7(2)	0.068 78(6)	−0.081 8(2)
	−0.385 7(3)	0.068 37(8)	−0.077 8(3)
C(5B)	−0.280 7(2)	0.090 56(7)	−0.089 6(2)
	−0.276 3(3)	0.089 9(1)	−0.087 2(3)
C(6B)	−0.180 7(2)	0.112 71(7)	0.027 6(2)
	−0.175 1(3)	0.112 8(1)	0.029 3(3)
C(7B)	−0.494 7(2)	0.043 05(7)	−0.208 4(2)
	−0.491 4(3)	0.042 0(1)	−0.203 4(3)
C(8B)	−0.072 6(2)	0.135 71(6)	0.283 9(2)
	−0.063 6(3)	0.137 25(8)	0.286 4(3)
C(9B)	−0.217 5(2)	0.199 95(6)	0.269 5(1)
	−0.213 7(3)	0.199 2(1)	0.277 8(4)
C(1C)	0.547 0(2)	0.110 89(6)	0.484 6(2)
	0.548 5(2)	0.111 47(8)	0.491 0(3)
C(2C)	0.677 7(2)	0.130 84(6)	0.537 9(2)
	0.680 1(3)	0.130 96(9)	0.543 4(3)
C(3C)	0.792 9(2)	0.106 74(6)	0.555 4(2)
	0.795 2(3)	0.106 43(9)	0.559 9(3)
C(4C)	0.780 7(2)	0.062 74(6)	0.519 9(2)
	0.780 4(3)	0.062 47(8)	0.522 8(3)
C(5C)	0.650 6-2)	0.043 20(6)	0.469 3(2)
	0.648 5(3)	0.043 38(9	0.473 4(3)
C(6C)	0.535 3(2)	0.066 64(4)	0.452 9(2)
	0.534 6(3)	0.067 19(9)	0.458 4(3)
C(7C)	0.903 5(2)	0.036 99(6)	0.530 7(2)
	0.901 9(3)	0.036 4(1)	0.532 2(4)
C(8C)	0.420 8(2)	0.134 05(6)	0.470 6(2)
	0.422 6(2)	0.135 24(8)	0.477 7(2)
C(9C)	0.442 8(2)	0.197 65(6)	0.333 4(2)
	0.442 1(3)	0.197 14(9)	0.332 5(3)
Solvent			
O(1D)	0.141 8(2)	0.236 08(5)	0.956 2(2)
	0.148 7(2)	0.235 92(7)	0.962 1(2)
C(1D)	0.131 4(3)	0.275 09(9)	0.757 5(4)
	0.137 9(4)	0.275 4(1)	0.761 0(5)
C(2D)	0.083 7(2)	0.241 15(6)	0.826 1(2)
	0.089 3(3)	0.240 93(9)	0.829 7(3)
C(3D)	−0.037 1(2)	0.214 16(8)	0.728 3(3)
	−0.033 6(4)	0.214 1(1)	0.730 2(4)
O(1E)	0.021 5(2)	0.217 01(8)	0.143 0(2)
	0.012 0(3)	0.217 4(1)	0.140 4(3)

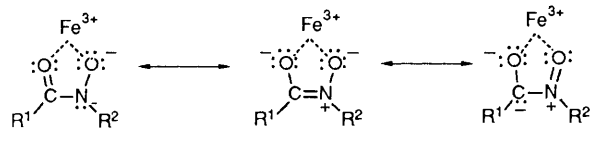

I II III

no significant changes in the geometry and dimensions of the methylphenyl rings are observed in either ligand on complexation.

Effect of the Interchange of the Hydroxamate C *and* N *Substituents on the Structure and Stability of Complexes* **1** *and* **2**.—The dimensional changes observed upon iron co-ordination indicate that the stability of the iron(III) hydroxamate chelate ring is dependent fundamentally on the strength of the two, largely ionic, Fe–O bonds, and, therefore, on the gain of electron density (and formal negative charge) by the carbonyl oxygen atom, O(1). The delocalization of electron density over the hydroxamate ring atoms is effected in general by the resonance and inductive interactions of the R^1 and R^2 substituents of the hydroxamate group, which influence: (1) the delocalization of the hydroxamate N(9) atom lone pair of electrons into the C(8)–N(9) bond and towards the carbonyl O(1) atom (resonance form **II**); and (2) the delocalization of electron density gained by deprotonation of the oxime O(2) atom into the N(9)–O(2) bond (resonance form **III**). The first effect, while resulting in a formal positive charge on the N(9) atom, leads to increased electron density on the carbonyl O(1) atom; the second both stabilizes this formal charge on N(9) and reduces the electron density on O(2), thereby levelling the charges on the hydroxamate O(1) and O(2) atoms. The significant shortening of C(8)–N(9) upon chelation shows the fundamental importance of resonance form **II**.

A comparison of the average values of structural parameters of the iron(III) hydroxamate chelate rings and the co-ordination spheres of complexes **1** and **2** is given in Table 6. The emphasis is placed on bond-distance differences, because they command relatively larger energy contributions than those involved in bond-angle or torsion-angle changes. The observed geometric differences arise largely from the relative influences of the CH_3 and $C_6H_4CH_3$ substituents when bonded to the oxime nitrogen atom N(9), rather than the carbonyl carbon atom C(8). In **2** the CH_3 group can stabilize delocalization of the nitrogen lone pair inductively (resonance form **II**), while in **1** the $C_6H_4CH_3$ substituent cannot stabilize this form inductively, acting instead as an electron-withdrawing group, thereby

Table 4 Bond distances (Å) for all non-hydrogen atoms in $[Fe(mpa)_3]$, $[Fe(mmb)_3]$ and $[Ga(mmb)_3]$; e.s.d.s are given in parentheses

		$[Fe(mpa)_3]$			$[Fe(mmb)_3]$			$[Ga(mmb)_3]$		
Parameter	Ligand	A	B	C	A	B	C	A	B	C
M–O(1)[a]		2.037(1)	2.067(1)	2.057(1)	2.045(1)	2.044(1)	2.045(1)	1.989(1)	1.985(2)	1.989(2)
M–O(2)		1.973(1)	1.966(1)	1.972(1)	1.978(1)	1.976(1)	1.995(1)	1.946(2)	1.944(2)	1.966(2)
C(8)–O(1)		1.269(2)	1.267(2)	1.269(2)	1.278(2)	1.277(2)	1.278(2)	1.279(2)	1.278(3)	1.275(2)
N(9)–O(2)		1.385(2)	1.382(2)	1.384(2)	1.378(1)	1.375(2)	1.378(2)	1.378(2)	1.374(2)	1.384(3)
C(8)–N(9)		1.322(2)	1.325(2)	1.323(2)	1.316(2)	1.310(2)	1.318(2)	1.313(3)	1.310(3)	1.313(3)
C(8)–C(R^1)[b]		1.489(2)	1.491(3)	1.495(3)	1.487(2)	1.491(2)	1.488(2)	1.492(3)	1.491(3)	1.493(3)
N(9)–C(R^2)[b]		1.435(2)	1.433(2)	1.427(2)	1.458(2)	1.455(2)	1.454(2)	1.456(3)	1.457(4)	1.459(3)
C(1)–C(2)		1.381(3)	1.388(2)	1.388(3)	1.398(2)	1.391(2)	1.399(2)	1.395(2)	1.392(3)	1.394(4)
C(1)–C(6)		1.387(3)	1.387(3)	1.388(2)	1.390(3)	1.388(2)	1.390(3)	1.389(4)	1.389(2)	1.393(4)
C(2)–C(3)		1.386(3)	1.384(3)	1.386(3)	1.387(2)	1.380(3)	1.389(2)	1.390(3)	1.391(4)	1.394(4)
C(3)–C(4)		1.386(3)	1.398(3)	1.390(2)	1.389(3)	1.388(2)	1.391(3)	1.388(4)	1.390(2)	1.393(4)
C(4)–C(5)		1.388(3)	1.384(3)	1.390(3)	1.393(2)	1.394(3)	1.391(3)	1.401(3)	1.399(4)	1.394(4)
C(4)–C(7)		1.511(3)	1.509(3)	1.510(3)	1.508(3)	1.507(3)	1.506(3)	1.509(3)	1.502(4)	1.503(4)
C(5)–C(6)		1.382(3)	1.388(3)	1.384(3)	1.386(2)	1.380(3)	1.382(2)	1.388(3)	1.381(4)	1.377(4)
Solvent										
C(1D)–C(2D)		1.494(3)			1.490(3)			1.489(4)		
C(2D)–C(3D)		1.491(3)			1.483(3)			1.487(4)		
O(4D)–C(2D)		1.205(3)			1.217(2)			1.227(3)		

[a] M = Trivalent metal ion. [b] In $[Fe(mpa)_3]$, C(R^1) = C(9) and C(R^2) = C(1); in $[Fe(mmb)_3]$ and $[Ga(mmb)_3]$, C(R^1) = C(1) and C(R^2) = C(9).

Table 5 Selected bond and torsion angles (°) for all non-hydrogen atoms with e.s.d.s in parentheses

		$[Fe(mpa)_3]$			$[Fe(mmb)_3]$			$[Ga(mmb)_3]$		
Parameter	Ligand	A	B	C	A	B	C	A	B	C
M–O(1)–C(8)[a]		114.2(1)	112.6(1)	113.9(1)	113.5(1)	112.9(1)	113.3(1)	111.9(1)	111.8(1)	112.1(2)
M–O(2)–N(9)		112.7(1)	112.1(1)	112.3(1)	112.8(1)	112.5(1)	112.4(1)	110.3(1)	110.0(1)	109.8(1)
O(1)–M–O(2)		78.33(4)	78.41(5)	77.95(5)	78.47(4)	78.81(5)	78.36(4)	81.26(6)	81.49(7)	81.26(7)
O(1)–C(8)–N(9)		118.0(1)	118.2(2)	117.6(2)	118.5(1)	118.9(1)	118.8(1)	118.9(2)	118.9(2)	119.5(2)
O(1)–C(8)–C(R^1)[b]		120.5(2)	121.3(2)	120.3(2)	119.2(1)	120.2(1)	119.0(2)	119.1(2)	119.8(2)	118.6(2)
C(R^1)–C(8)–N(9)[b]		121.5(2)	120.5(2)	122.0(2)	122.2(1)	120.9(1)	122.1(1)	122.0(2)	121.3(2)	121.9(2)
O(2)–N(9)–C(8)		116.2(1)	116.9(1)	116.5(1)	116.5(1)	116.9(1)	116.5(1)	117.2(2)	117.5(2)	117.1(2)
O(2)–N(9)–C(R^2)[b]		115.0(1)	114.6(1)	114.9(1)	113.4(1)	115.1(1)	114.0(1)	113.3(2)	114.9(2)	113.5(2)
C(R^2)–N(9)–C(8)[b]		128.8(1)	128.4(1)	128.6(2)	129.0(2)	127.6(1)	129.0(1)	128.7(2)	126.8(2)	129.1(2)
O(1)–C(8)–N(9)–O(2)		1.3(2)	0.5(3)	6.5(2)	2.3(2)	2.0(2)	1.8(2)	2.2(3)	2.6(2)	1.7(3)
M–O(1)–C(8)–N(9)		4.3(2)	9.5(2)	3.8(2)	0.7(2)	−1.4(2)	−6.9(2)	3.1(3)	1.5(2)	−4.2(2)
C(8)–O(1)–M–O(2)		−6.0(1)	−11.7(1)	−8.8(1)	−2.3(1)	0.3(2)	7.0(1)	−5.2(2)	−3.5(1)	3.9(1)
M–O(2)–N(9)–C(8)		−6.4(2)	−10.6(2)	−13.8(2)	−4.1(2)	−1.6(1)	4.4(1)	−6.4(2)	−5.3(2)	1.8(2)
C(R^1)–C(8)–N(9)–C(R^2)[b]		−0.8(3)	3.3(3)	11.6(3)	17.0(3)	−5.3(2)	10.9(2)	15.8(4)	−7.2(3)	7.7(3)
O(2)–N(9)–C(1)–C(6)		−63.0(2)	−53.6(2)[c]	47.3(2)	—	—	—	—	—	—
C(6)–C(1)–C(8)–O(1)		—	—	—	39.2(2)	−68.9(2)	42.5(2)	41.3(3)	−65.3(3)	44.9(2)

[a] M = Trivalent metal ion. [b] In $[Fe(mpa)_3]$, C(R^1) = C(9) and C(R^2) = C(1); in $[Fe(mmb)_3]$ and $[Ga(mmb)_3]$, C(R^1) = C(1) and C(R^2) = C(9). [c] Angle taken for O(2)–N(9)–C(1)–C(2).

reducing the extent of N(9) lone-pair delocalization into the C(8)–N(9) bond. This observation is also supported by the higher acidity of mmb compared to mpa and is reflected in the pK_a values of 8.50 and 8.81,[17,18] respectively.

As a natural consequence of these differences in the electronic interactions of the hydroxamate substituents, a number of important structural differences arise between **1** and **2** that are manifested in differences in the thermodynamic stabilities of the two chelates. First, the average C(8)–N(9) bond in **2** is 0.009 Å shorter than in **1** indicating a larger contribution of canonical form **II** in structure **2**. Secondly, the oxime N(9)–O(2) bonds are on the average 0.007 Å shorter in **2** than in **1**, suggesting greater importance of form **III** in structure **2**. Both of these effects should result in longer C(8)–O(1) bond distances in **2** when compared to **1**; this is indeed observed with the 0.010 Å increase in the C(8)–O(1) bond from 1.268(2) Å in **1** to 1.278(2) Å in **2**. The longer carbonyl bond in **2** is indicative of a greater negative formal charge on the O(1) atom, as compared with **1**. Viewed in other terms, the smaller difference between the average carbonyl bond distance and the average oxime bond length {|[C(8)–O(1)] − [N(9)–O(2)]|} in **2** [0.099(2) Å] as compared to **1** [0.116(2) Å] indicates that a larger formal negative charge resides on O(1) in **2** and that there is a greater equivalency of the negative charges on the hydroxamate oxygen atoms [O(1) and O(2)].

Another consequence of these observations is the expectation of stronger Fe–O(1) and weaker Fe–O(2) bonding interactions in complex **2** as compared to **1**. This is observed; the average Fe–O(1) bond is 0.009 Å shorter [2.045(1) *versus* 2.054(1) Å] and the Fe–O(2) bond is 0.007 Å longer [1.977(1) *versus* 1.970(1) Å] in **2** compared to **1**. Lastly, it would be expected that the distance from the Fe^{3+} ion to the centre of the trigonal face of O(1) atoms would be shorter in **2** [1.186(1) Å] than in **1** [1.227(1) Å]. All these observations indicate that, in general, the most stable iron(III) hydroxamate will be formed when both R^1 and R^2 substituents are donating, inductively and/or *via* resonance, electron density into the chelate ring, thus enhancing the negative charge on the carbonyl oxygen atom [O(1)],

Table 6 Comparison of selected average structural geometry (distances in Å, angles in °) for metal co-ordination with e.s.d.s in parentheses

	$[Fe(mpa)_3]$	$[Fe(mmb)_3]$	$[Ga(mmb)_3]$
Metal co-ordination sphere[a]			
Configuration	Λ,Δ-*cis*	Λ,Δ-*cis*	Λ,Δ-*cis*
M–O(1) face	1.227(1)	1.186(1)	1.148(1)
M–O(2) face	1.088(1)	1.058(1)	1.066(1)
Angle, M and centre of gravity between O trigonal planes	179.8(2)	178.3(1)	178.6(1)
Chelate ring[b]			
M–O(1)	2.054(1)	2.045(1)	1.988(2)
M–O(2)	1.970(1)	1.977(1)[c]	1.945(2)[c]
O(1)···O(2)	2.540(1)	2.550(1)	2.568(2)
Ligand bite[d]	1.26	1.27	1.31
Twist angle	35.57(5)	42.42(4)	46.97(9)
O(1)–M–O(2)	78.23(5)	78.54(4)	81.34(7)
C(8)–O(1)	1.268(2)	1.278(2)	1.277(2)
N(9)–O(2)	1.384(2)	1.377(2)	1.379(2)
N(9)–C(8)	1.324(2)	1.315(2)	1.312(3)
M–O(1)–C(8)	113.5(1)	113.2(1)	111.9(1)
M–O(2)–N(9)	112.4(1)	112.6(1)	110.0(1)
Σ angles around C(8)	359.9	359.9	360.0
Σ angles around N(9)	359.9	359.3	359.4

[a] Trigonal faced defined as:

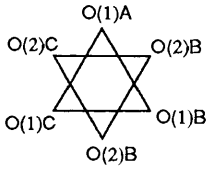

[b] The e.s.d. for the average value is given in parentheses; e.s.d.s for individual distances and angles are found in Tables 4 and 5, and are in the ranges 0.001–0.003 Å and 0.01–0.02°, respectively, for compounds **1**–**3**. [c] Average for M–O(2) for rings A and B only. [d] Defined as the ratio of the average O(1)···O(2) distance to the average Fe–O distance.

diminishing the charge on the ionic oxime oxygen [O(2)], and stabilizing the positive charge on the hydroxamate nitrogen atom [N(9)].

Structurally, the most stable complex is recognized as possessing: (1) the shortest C(8)–N(9) distances; (2) the smallest difference in C(8)–O(1) and N(9)–O(2) distances [|(N–O) – (C=O)|]}; (3) the smallest difference in Fe–O(1) and Fe–O(2) distances (|Δ(Fe–O)|); and (4) the smallest difference in the distances between the Fe^{3+} ion and the planes of the oxime and carbonyl oxygen atoms [$|\Delta(Fe–O)_{face}|$] (Table 7). The last two characteristics should be the most reliable predictors of structural stability since they involve the parameters of Fe^{3+} ion which can be determined most accurately. These structure–stability criteria indicate that complex **2** is structurally more stable than **1**. The correlation can be extended further when the criteria are applied to other structures, such as tris-[*N*-(4-cyanophenyl)acetohydroxamato]iron(III) $[Fe(cnpa)_3]$, a complex similar to **1**, except that the N(9)-substituted 4-cyanophenyl substituent is more strongly electron withdrawing than is the 4-methylphenyl group of mpa.[9] The comparison (Table 7) indicates that $[Fe(cnpa)_3]$ is structurally less stable than $[Fe(mpa)_3]$ **1**. A similar set of criteria have been used in a discussion of the structures of natural trihydroxamate-type siderophores.[8]

These conclusions, which correlate structural parameters with relative chelate stability, are supported by thermodynamic observations. The solution studies of Brink and Crumbliss[20] indicate that the first stepwise equilibrium constants (K_{f1}) for the reactions leading to the formation of the monohydroxamato iron(III) complexes (in general) have values of 1441, 294 and 54 for the ligands (HL), Hmmb, Hmpa and Hcnpa, respectively;

$$[Fe(H_2O)_6]^{3+} + HL(aq) \rightleftharpoons [FeL(H_2O)_4]^{2+} + H_3O^+(aq) + H_2O(l) \quad (1)$$

this order is the same as predicted from the structural results. To bring these values on to an absolute scale the contribution of hydrolysis of the different hydroxamic acids should be taken into account. Using literature values,[20] it is calculated that the $[Fe(mmb)(H_2O)_4]^{2+}$ complex is 2.1 kJ mol^{-1} more stable than its mpa counterpart. The energy difference for the two tris complexes can be expected to be even larger.

Geometric Changes upon Replacement of the Fe^{3+} *in Complex* **2** *with* Ga^{3+}.—The crystal structures of the complexes of mmb with Fe^{3+} and Ga^{3+}, **2** and **3**, are isomorphous (Table 1). In comparing their structures (Tables 4–7) the most notable differences in geometry occur in the metal co-ordination sphere about the Ga^{3+} ion. In **3**, the Ga–O(1) and Ga–O(2) bond distances are significantly shorter than in **2** [average of 1.988(2) and 1.945(2) Å in **3**, *versus* 2.045(1) and 1.977(1) Å in **2**]. This change is anticipated since the effective ionic radius for six-co-ordinate d^{10} Ga^{3+} of 0.62 Å is slightly smaller than that of the six-co-ordinate d^5 high-spin Fe^{3+} of 0.65 Å. As a consequence of the shorter Ga–O bonds in **3** there is a 2–3° increase in the O(1)–Ga–O(2) angles and a 0.04 increase in the ligand bite when compared to structure **2** (Table 6).

The relative structural stabilities of $[Fe(mmb)_3]$ and $[Ga(mmb)_3]$ were evaluated by applying the criteria developed in the previous section. The observations are summarized in Table 7. While the value of |(N–O) – (C=O)| is the same for the two chelates and the C(8)–N(9) bond is slightly shorter in **3**, the two most important and sensitive criteria, however, clearly indicate the greater stability of the $[Ga(mmb)_3]$ structure relative to its isomorphous iron(III) complex. That is, the observed values of |Δ(M–O)| [0.043(2) for **3**, 0.068(1) Å in **2**] and $|\Delta(M–O)_{face}|$ (0.082 in **3**, 0.128 Å in **2**) are significantly smaller in structure **3** compared to **2**. These observations clearly indicate that, structurally, the tris(hydroxamato)-gallium(III) complex is more stable than the corresponding iron(III) compound.

The same criteria used to distinguish the relative structural stability of complexes **2** and **3** can be used to compare the natural siderophore ferrichrome A with its isomorphous aluminium(III) analogue for which relatively accurate structures are available.[19] All four criteria (Table 7) indicate the aluminium(III) structure to be more stable than the iron(III) structure. Comparing alumichrome A with $[Ga(mmb)_3]$, three of the four criteria indicate the aluminium(III) structure to be more stable than the gallium(III) complex. These results indicate that structurally the stabilities of hydroxamatometal(III) complexes follow the order $Al^{3+} > Ga^{3+} > Fe^{3+}$.

It might appear that these conclusions, drawn from molecular structural data, are in direct conflict with known solution behaviour and thermodynamic observations of iron(III) hydroxamate chemistry. In solution, the formation of the tris(hydroxamato)iron(III) complex is given by the reaction (2) described

$$Fe^{3+}(aq) + 3L^-(aq) \rightleftharpoons [FeL_3](aq) \quad (2)$$

by the overall formation constant (3). Experimental values of

$$\beta_3 = [FeL_3]/[Fe^{3+}][L^-]^3 \quad (3)$$

the thermodynamic equilibrium constants (β_3) for chelates **2** and **3** have not been determined. It is generally accepted, however, that tris(hydroxamato)iron(III) complexes exhibit characteristic values of β_3 of the order of 10^{28} dm^9 mol^{-3}, while those for the corresponding derivatives of Ga^{3+} and Al^{3+} are

Table 7 Summary of structure–stability criteria[a] applied to some hydroxamate complexes of Fe^{3+}, Ga^{3+} and Al^{3+}

Parameter/Å	$[Fe(cnpa)_3]$[b]	$[Fe(mpa)_3]$	$[Fe(mmb)_3]$	$[Ga(mmb)_3]$	Alumichrome A[c]	Ferrichrome A[c]
$\lvert\Delta(M-O)\rvert$	0.103(2)	0.084(1)	0.068(1)	0.043(2)	0.024(2)	0.053(4)
$\lvert\Delta(M-O)_{face}\rvert$[d]	0.143	0.139	0.128	0.082	0.040	0.092
$\lvert(N-O) - (C=O)\rvert$	0.114(3)	0.116(2)	0.099(2)	0.098(2)	0.084(4)	0.107(5)
C–N	1.328(3)	1.324(2)	1.315(2)	1.312(3)	1.315(5)	1.326(7)

[a] See text for explanation. [b] From ref. 9. [c] From ref. 20. [d] $\Delta\{[M-O(1)_{face}] - [M-O(2)_{face}]\}$.

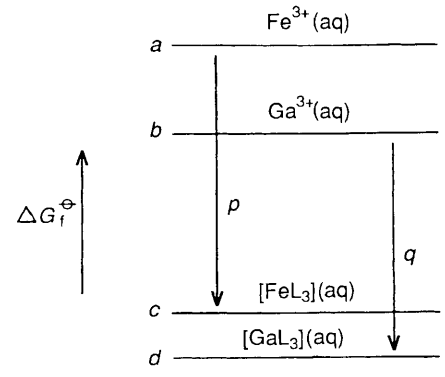

Fig. 5 Schematic drawing showing the relativity energy levels of the aquated and complexed (L = hydroxamate ligand) Fe^{3+} and Ga^{3+} ions

smaller: 10^{26} and 10^{22} dm^9 mol^{-3} respectively.[6,7,21] Recently, the pH-dependent stability constants for complexes of Ga^{3+} and Fe^{3+} with several catechol amides were reported,[22,23] indicating that the iron(III) chelates have β_3 values 10^3–10^5 times larger than those of their gallium counterparts. It is also known that $Fe^{3+}(aq)$ can easily displace Ga^{3+} ions from tris(hydroxamato)gallium(III) complexes, *i.e.* reaction (4) is spontaneous.[7]

$$Fe^{3+}(aq) + [GaL_3](aq) \rightleftharpoons Ga^{3+}(aq) + [FeL_3](aq) \quad (4)$$

There is a simple explanation for the apparent contradiction. Qualitatively, the conflict is resolved by realizing that the thermodynamic observations measure the relative values of the free energies of the formation of *both* the complex and the constituent ions (metal and ligand), while the conclusion advanced for the structure is an absolute one for only the complex. This can be stated in a more quantitative way. The complexes $[Fe(mmb)_3]$ and $[Ga(mmb)_3]$ have isomorphous structures, and therefore their entropies are closely similar. As a consequence, the greater structural stability of the gallium(III) complexes can be translated into a larger (more negative) value for the ΔG_f° of $[GaL_3]$ (point *d* in Fig. 5) than for $[FeL_3]$ (point *c* in Fig. 5). This difference, however, is more than compensated for by the much larger difference in free energy of formation of the aqueous ions[24] $\{\Delta G_f^\circ[Fe^{3+}(aq)] = -10.6$ kJ mol^{-1}, $\Delta G_f^\circ[Ga^{3+}(aq)] = -159.1$ kJ mol^{-1}; points *a* and *b*, Fig. 5$\}$. If it is assumed that the difference between free energies *c* and *d* is smaller than that between energies *a* and *b*, then $|p| > |q|$, realizing that the ligand is the same in the two compounds. It is the values of the free-energy differences *p* and *q* which determine the magnitude of the formation constants, *i.e.* the larger the absolute value of *p* or *q*, the larger is the formation constant. It is, therefore, the much lower free energy of formation of $Ga^{3+}(aq)$ compared to $Fe^{3+}(aq)$ which determines the smaller β_3 value of the $[Ga(mmb)_3]$ complex in comparison to the one for the $[Fe(mmb)_3]$ compound despite the larger structural stability of the former. The same argument explains the observation that Fe^{3+} replaces Ga^{3+} in hydroxamate complexes.

An identical argument can be made for aluminium(III) hydroxamate complexes. In this case, the $[AlL_3](aq)$ complex will have an even larger, more negative, value for ΔG_f° than energy *d*, in Fig. 5, but again, this is more than compensated for by the much larger negative free energy of formation of the aquated Al^{3+} ion $\{\Delta G_f^\circ[Al^{3+}(aq)] = -485.7$ kJ $mol^{-1}\}$.[24] These arguments, therefore, support the thermodynamic observation that $\beta_3[FeL_3] > \beta_3[GaL_3] > \beta_3[AlL_3]$ for hydroxamato ligands and the observation that $Fe^{3+}(aq)$ displaces both Ga^{3+} and Al^{3+} in hydroxamate complexes of these ions, while no contradiction exists with the structural results.

Summary and Conclusion

In summary, structural data obtained from accurate, high-angle single-crystal X-ray diffraction studies of related and/or isomorphous tris(hydroxamato)-iron(III) and -gallium(III) complexes have shown that the geometry and stability of the unsymmetrical five-membered metal(III) hydroxamate chelate ring is dependent on the electronic influences of the hydroxamate substituents and that the most stable chelate ring will result when both substituents donate electron density. Further, the absolute stabilities of the complexes of Fe^{3+}, Ga^{3+} and Al^{3+} can be determined using a set of structure–stability criteria which indicate these stabilities follow the sequence $Al^{3+} > Ga^{3+} > Fe^{3+}$. However, the thermodynamic stability is determined not only by the free energy of formation of the complexes but also by the free energies of formation of the aqueous ions; it appears that the latter clearly predominate, thereby explaining why the formation constants follow the order $Fe^{3+} > Ga^{3+} > Al^{3+}$, instead. These observations will be an important consideration in the design of ligands which are specific for Al^{3+} or Ga^{3+} compared to Fe^{3+}.

Experimental

All chemicals were used as purchased {iron(III) acetylacetonate, $[Fe(acac)_3]$, and $Ga(NO_3)_3$ (Aldrich)}. *N*-(4-Methylphenyl)-acetohydroxamic acid was a gift from Dr. A. L. Crumbliss, Duke University; *N*-methyl-4-methylbenzohydroxamic acid was prepared and purified as previously described.[12]

Spectra.—Proton ^1H NMR spectra were measured using a Varian XL (300 MHz) spectrometer. Fast-atom bombardment (FAB) mass spectra were obtained using a VG Analytical ZAB E double-focusing spectrometer; samples, dispersed in various matrices, were ionized by bombardment with 8 kV xenon atoms.

Preparations.—The ligand Hmpa (0.025 g, 0.15 mmol) was dissolved in acetone (4 cm^3); a solution of $[Fe(acac)_3]$ (0.018 g, 0.05 mmol) in acetone (4 cm^3) was added dropwise over 10 min, and the reaction mixture was stirred at 50 °C for 10 h, followed by 18 h of stirring at room temperature. Washing the resulting oil with diethyl ether followed by evaporation yielded a red-brown powder. The sample was chromatographed on a 1.5 × 19 cm column of Sephadex LH-20 with C_2H_5OH; homogeneity of the red-brown fractions was assessed by silica gel TLC using $CHCl_3$–CH_3OH–hexane (2:2:5, v/v/v). Rectangular crystals suitable for X-ray studies were obtained by slow precipitation of complex **1** from dry acetone using cyclopentane at −7 °C.

The FAB mass spectrum in a thioglycerol matrix exhibited the following important fragmentations: *m/z* 132 (100, base, $C_9H_{10}N^+$), 133 (10.8, $M + 1$ peak of *m/z* 132), 150 (22.7, $C_8H_9NO_2^+$), 220 {14.6, $[Fe(mpa)]^+$}, 384 {80.5, $[Fe(mpa)_2]^+$}, 549 {10, $[Fe(mpa)_3] - H^+$}, 604 {25.7, $[Fe_2(mpa)_3]^+$}, 824 {1.5, $[Fe_3(mpa)_4]^+$} and 932 {4.4%, $[Fe_2(mpa)_5]^+$}.

$[Fe(mmb)_3]$ **2**. The complex $[Fe(acac)_3]$ (0.025 g, 0.07 mmol) in acetone (10 cm^3) was added dropwise over 10 min to a solution of Hmmb 0.039 g, 0.24 mmol in acetone (7 cm^3) and stirred for 24 h at 40 °C. Repeated addition and evaporation of diethyl ether (2 cm^3) converted the resulting oil into a red-brown solid. The sample, in ethanol, was applied to a 1.5 × 22 cm bed of Sephadex LH-20 (Pharmacia) and eluted with ethanol. Purity was assessed chromatographically by elution on silica gel TLC plates (E. Merck) eluted with $CHCl_3$–hexane–CH_3OH (1:1:1, v/v/v). Prismatic crystals of compound **2** suitable for X-ray diffraction studies were grown from acetone solutions equilibrated with cyclopentane at 4 °C. They were unstable at room temperature.

The FAB mass spectrum in thioglycerol yielded the following spectrum: *m/z* 220 {3.4, $[Fe(mmb)]^+$}, 384 {100 base, $[Fe(mmb)_2]^+$}, 385 {22.9, $[Fe(mmb)_2] - H^+$}, 549 {7, $[Fe(mmb)_3] - H^+$}, 604 {22.1, $[Fe_2(mmb)_3] - H^+$} and 932 {9%, $[Fe_2(mmb)_5]^+$}.

$[Ga(mmb)_3]$ **3**. A suspension of $NaHCO_3$ (0.624 g, 7.5 mmol) in CH_3OH (25 cm^3) was slowly added to freshly crystallized Hmmb (0.600 g, 3.6 mmol) in CH_3OH (20 cm^3). Then, $Ga(NO_3)_3$ (0.258 g, 1.0 mmol) in CH_3OH (7 cm^3) was slowly added, followed by continuous stirring for 3 h at 65 °C and then for 20 h at 21 °C. The pale yellow product was evaporated to dryness, redissolved in ethanol (3 cm^3), and chromatographed on a bed of Sephadex LH-20 (2.5 × 48 cm) which had been previously deferriated. Fractions containing complex **3** were spotted on filter paper, visualized with 2% $FeCl_3$ in 0.1 mol dm^{-3} HCl, pooled and lyophilized. Colourless crystals were obtained from acetone solutions equilibrated with cyclopentane and a few drops of water at −6 °C. They were unstable at room temperature due to loss of solvent of crystallization.

The ^1H NMR (300 MHz) spectrum of $(CD_3)_2SO$ gave the expected chemical shifts relative to $SiMe_4$ [N–CH_3 protons, s, δ 2.37; *o*-phenyl protons, d, δ 7.40 (J = 7.1 Hz); *m*-phenyl protons, d, δ 7.45 (J = 7.1 Hz); *p*-methyl protons, s, δ 3.42], except that they were shifted slightly downfield from those observed for the free ligand [δ 2.33; 7.21 (J = 7.9); 7.53 (J = 8.03 Hz); 3.24; and N–OH proton, 9.958]. The FAB mass spectrum of $[Ga(mmb)_3]$ dispersed in a matrix of dithioerythritol–dithiothreitol (1:5, v/v) in CH_3OH yielded the following high-molecular-weight fragments: *m/z* 397 {100, $[Ga(mmb)_2]^+$ for ^{69}Ga}, 399 {68.2, $[Ga(mmb)_2]^+$ for ^{71}Ga}, 562 {0.8, $M + 1$ for $[^{69}Ga(mmb)_3]$}, 958 {3.4, $[^{69}Ga_2(mmb)_5]$}, 960 {4.2, $[^{69}Ga^{71}Ga(mmb)_5]$} and 962 {2.9, $[^{71}Ga_2(mmb)_5]$}.

X-Ray Structure Determination.—Crystal data and experimental parameters pertaining to the structure solution and refinement for compounds **1**–**3** are in Table 1. Due to their instability, the crystals used for data collection were generally mounted quickly onto glass fibres with vacuum grease (Celvacene Medium, Consolidated Vacuum Corp.) and transferred into the cold nitrogen stream (−135 °C). Diffraction data were collected with an Enraf-Nonius CAD-4 automatic diffractometer equipped with a liquid-nitrogen low-temperature device that maintains crystal temperatures at −135(2) °C. Cell parameters were obtained by a least-squares fit to the 2θ and −2θ values of at least 48 high-angle reflections. Space groups were determined from systematic absences of 0*k*0 reflections, where *k* is odd, and for the *h*0*l* plane, when *h* is odd. Lorentz and polarization corrections were made. The orientation of the crystal was monitored by measuring three control reflections every 200 measurements; a new orientation matrix calculated from a list of 24 reflections was computed if an angular change of more than 0.1° was observed. For compounds **1** and **3**, data were collected using the θ–2θ scan mode and reduced with a set of peak-profile analysis programs.[25] Six monitor reflections were used for anisotropic, intensity-dependent, and scattering angle-dependent scaling. The maximum fractional error $\sigma(k)/k$, where k is the scaling factor, was 1.0% for complex **1** and 3.5% for **3**. For compound **2**, data were collected using ω scans and reduced with the standard Enraf-Nonius data-reduction programs. The three monitor reflections showed a maximum variation of 2.9%. Absorption corrections were made for all three crystals. Scattering factors for C, N and O were taken from Cromer and Mann,[26] for Fe^{3+} and Ga^{3+} from ref. 27, and for H from Stewart *et al.*[28]

The structures of compounds **1** and **2** were solved from three-dimensional Patterson syntheses, which revealed very distinct Fe–Fe vectors; the complete structures, including location of all hydrogen atoms, were elucidated from successive Fourier difference syntheses, using the SHELX 76 program.[29] All non-hydrogen atoms were refined anisotropically and hydrogen atoms isotropically using full-matrix least squares in which the quantity $\Sigma w(|F_o| - |F_c|)^2$ was minimized; refinements were discontinued when the maximum shift-to-error ratios (Δ/σ) made less than 0.07. Final Fourier difference syntheses showed residual electron density between 0.52 and −0.22 e $Å^{-3}$, and 0.36 and −0.26 e $Å^{-3}$, for **1** and **2**, respectively, with the maximum appearing along the Fe–O bonds.

The structure of complex **3** was found to be isomorphous with that of **2**; cell dimensions of **2** and **3** agreed within 0.3%. The structure of **3** was solved using the coordinates of the atoms of $[Fe(mmb)_3]\cdot H_2O\cdot Me_2CO$, and refined as described above using full-matrix least-squares methods with Δ/σ less than 0.001. A final Fourier difference synthesis showed maximum and minimum peak heights between +1.08 (along the Ga–O bonds) and −0.62 e $Å^{-3}$.

Final atomic coordinates for the non-hydrogen atoms, including solvent, in structures **1**–**3** are given in Tables 2 and 3, respectively.

Additional material available from the Cambridge Crystallographic Data Centre comprises H-atom coordinates, thermal parameters and remaining bond lengths and angles.

Acknowledgements

This work was supported by a grant from the National Institute for General Medical Sciences (GM-21822). We also thank Dr. Alvin L. Crumbliss, Department of Chemistry, Duke University for the gift of a sample of *N*-(4-methylphenyl)acetohydroxamic acid, and Tom Karns, Analytical Services, Department of Chemistry and Biochemistry, The University of Oklahoma for assistance in obtaining the FAB mass spectra. An academic exchange program between The University of Oklahoma and The Technical University of Berlin, Germany, is also acknowledged.

References

1 J. B. Neilands, *Adv. Inorg. Biochem.*, 1983, **5**, 137.
2 K. N. Raymond, G. Müller and B. F. Matzanke, *Top. Curr. Chem.*, 1984, **123**, 49
3 R. C. Hider, *Struct. Bonding (Berlin)*, 1984, **58**, 25.
4 G. Winkelmann and H-G. Huschka, in *Iron Transport in Microbes, Plants and Animals*, eds. G. Winkelmann, D. van der Helm and J. B. Neilands, VCH, New York, 1987, p. 317.
5 H. Kehl, *Chemistry and Biology of Hydroxamic Acids*, Karger, New York, 1982.
6 G. Anderegg, F. L'Eplattenier and G. Schwarzenbach, *Helv. Chim. Acta*, 1963, **46**, 1400.
7 T. Emery and P. B. Hoffer, *J. Nucl. Med.*, 1980, **21**, 935.
8 D. van der Helm, M. A. F. Jalal and M. B. Hossain, in *Iron Transport in Microbes, Plants and Animals*, eds. G. Winkelmann, D. van der Helm and J. B. Neilands, VCH, New York, 1987, p. 135.
9 R. Mocharla, D. R. Powell, C. L. Barnes and D. van der Helm, *Acta Crystallogr., Sect. C*, 1983, **39**, 868.

10 R. Mocharla, D. R. Powell and D. van der Helm, *Acta Crystallogr., Sect. C*, 1984, **40**, 1369.
11 D. R. Powell and D. van der Helm, *Acta Crystallogr., Sect. C*, 1987, **43**, 493.
12 A. Dietrich, D. R. Powell, D. L. Eng-Wilmot, M. B. Hossain and D. van der Helm, *Acta Crystallogr., Sect. C*, 1990, **46**, 816.
13 B. A. Borgias, S. J. Barclay and K. N. Raymond, *J. Coord. Chem.*, 1986, **15**, 109.
14 B. Monzyk and A. L. Crumbliss, *J. Am. Chem. Soc.*, 1982, **104**, 4921.
15 D. van der Helm and M. Poling, *J. Am. Chem. Soc.*, 1976, **98**, 82.
16 M. B. Hossein, D. van der Helm and M. Poling, *Acta Crystallogr., Sect. B*, 1983, **39**, 258.
17 C. P. Brink and A. L. Crumbliss, *J. Org. Chem.*, 1982, **7**, 1171.
18 C. P. Brink, L. L. Fish and A. L. Crumbliss, *J. Org. Chem.*, 1985, **50**, 2277.
19 D. van der Helm, J. R. Baker, R. A. Loghry and J. D. Ekstrand, *Acta Crystallogr., Sect. B*, 1981, **37**, 323.
20 C. P. Brink and A. L. Crumbliss, *Inorg. Chem.*, 1984, **23**, 4708.
21 A. L. Crumbliss and J. M. Garrison, *Comments Inorg. Chem.*, 1988, **8**, 1.
22 V. L. Pecoraro, F. L. Weitl and K. N. Raymond, *J. Am. Chem. Soc.*, 1981, **103**, 5133.
23 M. J. Kappel, V. L. Pecoraro and K. N. Raymond, *Inorg. Chem.*, 1985, **24**, 2447.
24 W. M. Latimer, *The Oxidation States of the Elements and their Potentials in Aqueous Solutions*, Prentice Hall, New York, 1952.
25 R. H. Blessing, *Crystallogr. Rev.*, 1987, **1**, 3.
26 D. T. Cromer and J. B. Mann, *Acta Crystallogr., Sect. A*, 1968, **24**, 321.
27 J. A. Ibers and W. C. Hamilton, in *International Tables for X-Ray Crystallography*, Kynoch Press, Birmingham, 1962, vol. 3, p. 202.
28 R. F. Stewart, E. R. Davidson and W. T. Simpson, *Chem. Phys.*, 1965, **42**, 3175.
29 G. M. Sheldrick, SHELX 76, Program for Crystal Structure Determination, Cambridge University, 1976.

Received 26*th July* 1990; *Paper* 0/03418E